**Chapter one** 

Introduction

#### 1.1 INTRODUCTION

**Breast cancer** is the most common invasive cancer in females worldwide. It accounts for 16% of all female cancers and 22.9% of invasive cancers in women. 18.2% of all cancer deaths worldwide [1].

Early detection is the key to improve breast cancer prognosis, and mammography is considered the modality of choice for the early detection of breast carcinomas [2]. Mammography is an imaging procedure that allows the application of low dose radiation (usually around 0.7 mSv) in order to obtain an image of the female breast for medical examination.

#### 1.2 OBJECTIVES

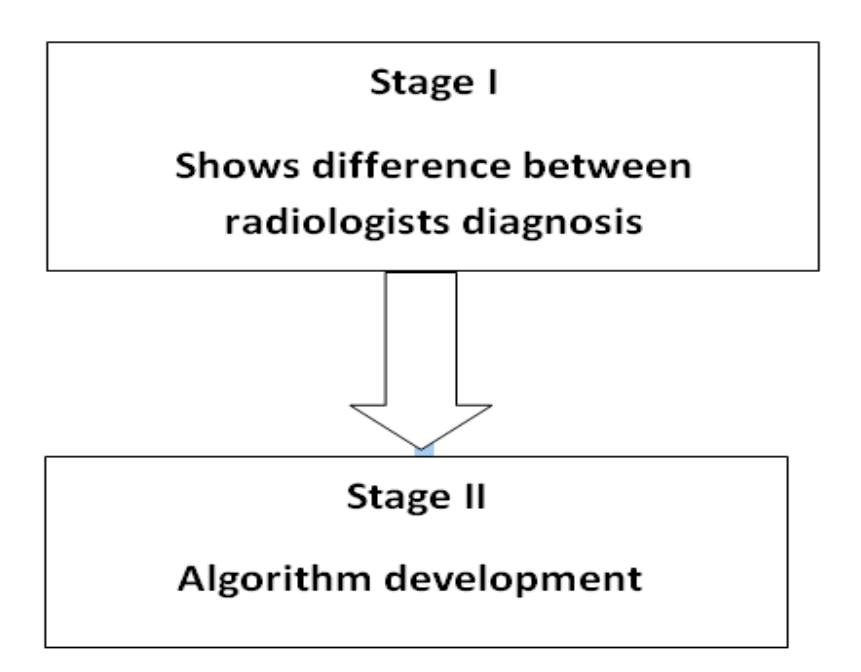
In breast cancer screening radiologists select a small percentage of women for referral based on suspicious abnormalities in their mammograms. To maintain high specificity, radiologists do not refer all abnormalities they see. Consequently, not all cancers initially detected are acted upon because SFM (Screen-film mammography) is currently the commonly type of mammography used in the medical facilities in Sudan, the eminent benefits of DM (Digital mammography) modalities incorporating image processing and CAD (Computer-aided detection) diagnosis technologies are deficient.

#### The specific objectives of this project are to:

- 1. To show and prove the difference of the interpretation of mammographic images by radiologists.
- 2. Attempt to develop CAD techniques that aim to provide a second option diagnosis for radiologist.
- 3. Reduce health care costs by decreasing the need for follow-up procedures such as biopsy.

#### 1.3 THESIS LAYOUT

The project is divided into two stages, as follows:



In the first stage: Twenty digital mammogram images were downloaded from MIAS database. Each image contains one or two benign tumors to prove the variability among radiologists to detect benign tumors in the images.

The second stage was attempted to develop the algorithm required for the detection of benign tumors in digital mammograms. The analysis of mammograms and the proposed algorithm will be carried out using Matrix Laboratory (MATLAB)

# Chapter two Theoretical Background

#### 2.1ANATOMY AND PHYSIOLOGY OF THE BREAST

The exterior of all humans' breasts are basically the same; however, the size, shape, and function of breasts vary significantly between the sexes. The key parts of the female breast include:

- **a. Breast**: The larger, more pronounced part of the breast is typically visible through clothing. Some cultures associate breast size with sexuality, and others view a woman's breast size as a sign of maturity and fertility.
- **b. Areola**: This circular area around the nipple typically has darker or deeper pink colored skin. The color can change over time due to hormonal changes associated with menstruation, menopause, and pregnancy.
- **c. Nipple**: The protruding tip of the breast, the nipple is where breast milk ultimately flows from and exits the body. It is also the site of many nerve endings. Typically, each breast has one, but in rare cases more than one may be present.

#### 2.1.1 BREAST ANATOMY

Anatomically, each breast has 15 to 20 sections, called lobes that are arranged like the petals. Each lobe has many smaller lobules, which end in dozens of tiny bulbs that can produce milk. The lobes, lobules, and bulbs are all linked by thin tubes called ducts. These ducts lead to the nipple in the center of a dark area of skin called the areola, resulting in a darkened appearance as shown in Figure (2.1), Fat fills the spaces between lobules and ducts. There are no muscles in the breast, but muscles lie under each breast and cover the ribs [3].

Each breast also contains blood vessels and vessels that carry lymph. The lymph vessels lead to small bean-shaped organs called lymph nodes, clusters of which are found under the arm, above the collarbone, and in the chest, as well as in many other parts of the body.

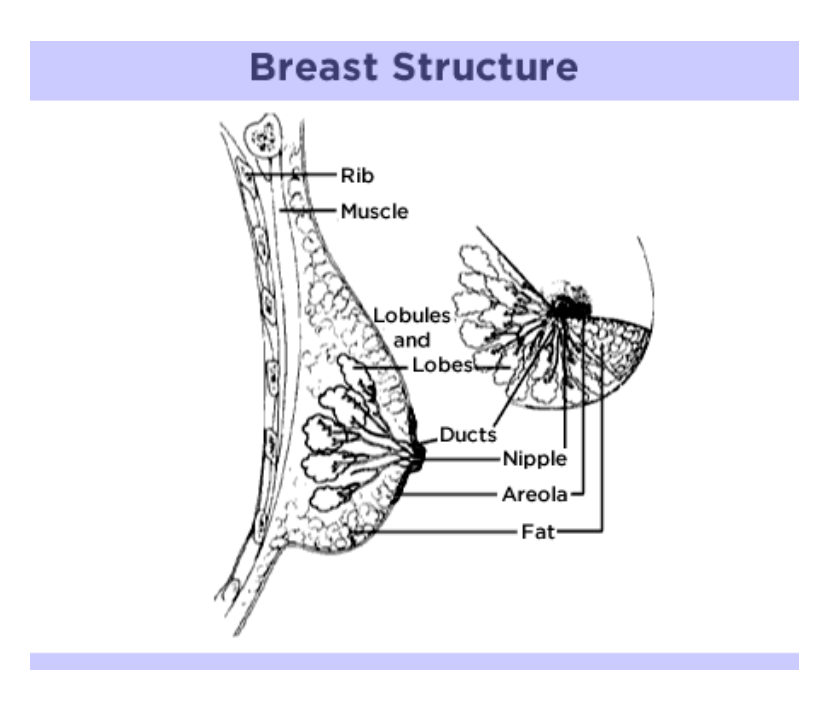


Figure 2.1 shows the structure of the breast [3].

#### 2.1.2 BREAST PHYSIOLOGY

The breast's main function is to produce, store and release milk to feed a baby. Milk is produced in lobules throughout the breast when they are stimulated by hormones in a woman's body after giving birth. The ducts carry the milk to the nipple. Milk passes from the nipple to the baby during breast-feeding.

#### 2.1.2.1 HORMONES OF LACTASION

The complex physiology of breastfeeding includes a delicate balance of hormones. The four hormones that help breasts to make milk are:

- a. Estrogen.
- b. Progesterone.
- c. Prolactin.
- d. Oxytocin.

The body naturally knows how to adjust the level of these hormones to help the breasts to make milk, as shown in the Figure (2.2).

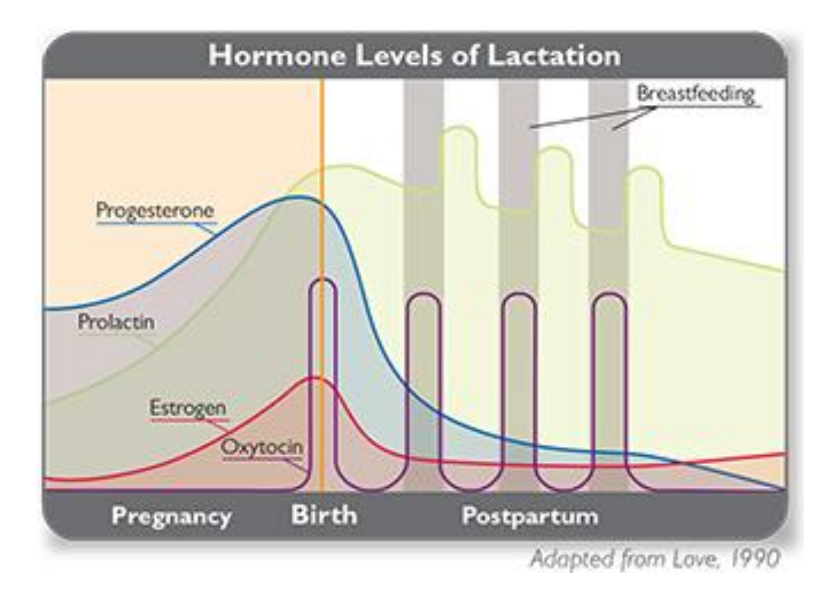


Figure 2.2 shows the hormone levels of location [4].

#### 2.2 BREAST CANCER

Women are more prone to problems with their breasts. These problems can include:

- 1. Breast cancer.
- 2. Benign breast lumps.
- 3. Mastitis or breast infection.
- 4. Virginal breast hypertrophy or premature development of large breasts.

**Breast cancer** is a type of cancer originating from breast tissue, most commonly from the inner lining of milk ducts or the lobules that supply the ducts with milk. Cancers originating from ducts are known as ductal carcinomas, while those originating from lobules are known as lobular carcinomas as shown in Figure (2.3).

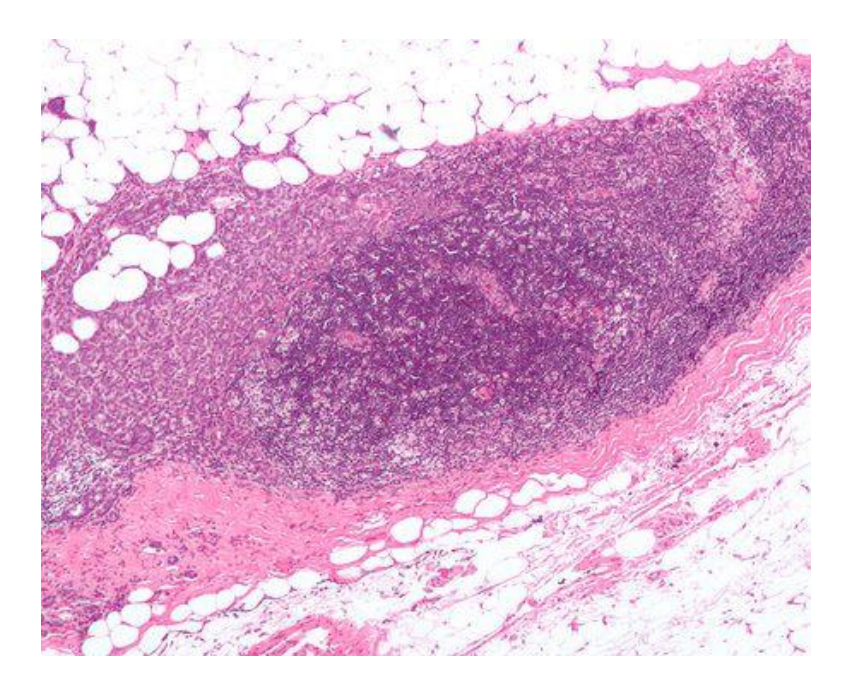


Figure 2.3 shows the Micrograph a lymph node invaded by ductal breast carcinoma [5].

Worldwide, breast cancer accounts for 22.9% of all cancers (excluding non-melanoma skin cancers) in women. Breast cancer is more than 100 times more common in women than in men, although men tend to have poorer outcomes due to delays in diagnosis [6].

The characteristics of the cancer determine the treatment which may include surgery, medications (hormonal therapy and chemotherapy) and radiation.

#### 2.3 MAMMOGRAPHY

Mammography is method that allows the early detection of breast cancer. The detection process involves diagnosing the mammograms based on the identification of areas of high intensities that indicate the presence of either benign or malignant tumors [7].

There are two main types of mammography: film-screen mammography and digital mammography DM, also called full-field digital mammography or FFDM. The technique for performing them is the same. What differs is whether the images take the form of photographic films or of digital files recorded directly onto a computer [6].

#### 2.4 DIGITAL MAMMOGRAPHY

**Digital mammography**, also called full-field digital mammography (FFDM), is a mammography system in which the x-ray film is replaced by electronics that convert x-rays into mammographic pictures of the breast, as shown in Figure (2.4). These systems are similar to those found in digital cameras and their efficiency enables better pictures with a lower radiation dose. These images of the breast are transferred to a computer for review by the radiologist and for long term storage. The patient's experience during a digital mammogram is similar to having a conventional film mammogram.

Most centers now use digital mammography. Because digital images are viewed on a computer, they can be lightened or darkened, and certain sections can be enlarged and looked at more closely. The ability to control images on a computer makes digital mammography more accurate than film mammography for some women. In general, digital mammography is better at finding breast cancer in women who:

- a) Are premenopausal or peri-menopausal.
- b) Are under age 50.
- c) Have dense breast tissue.

For women who do not fall in one of the above groups, film and digital mammography are similar in their ability to find breast cancer early [3].



Figure 2.4 shows the digital mammography [8].

#### 2.5 BENIGN TUMOR

Masses are three-dimensional lesions which may represent a localizing sign of breast cancer. They are described by their location, size, shape, margin characteristics, X-ray attenuation (radio density), effect on surrounding tissue, and any other associated findings (i.e. architectural distortion, associated calcifications, skin changes). Depending on the morphologic criteria of the mass, the likelihood of malignancy can be established. A round, oval, or lobulated mass with sharply defined borders has a high likelihood of being benign, as shown in Figure (2.5) [9].

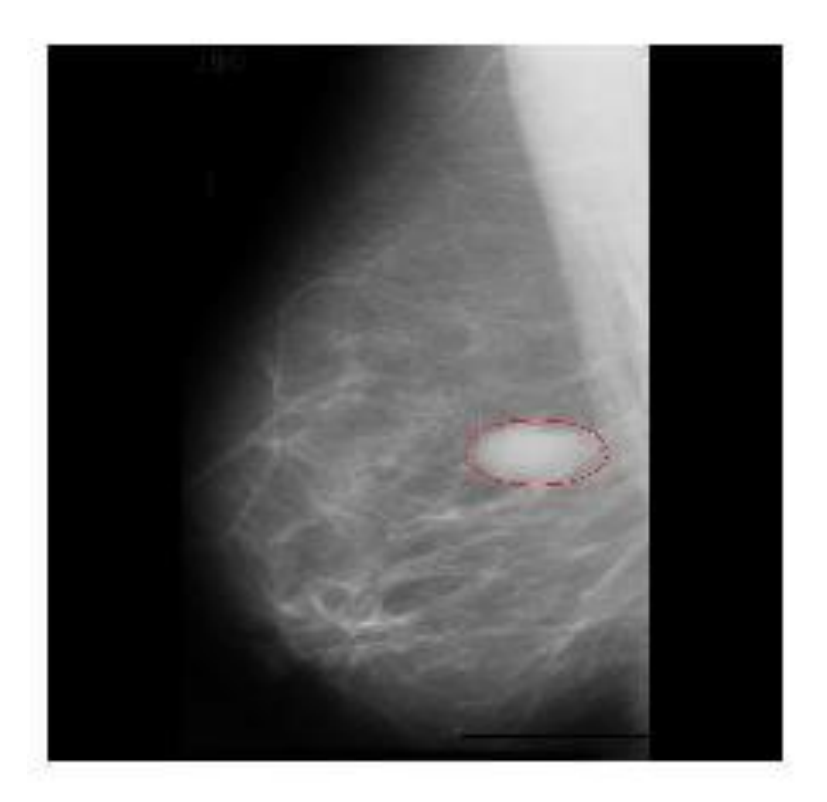


Figure 2.5 shows the Mammogram with benign mass [9].

A mammographic image may contain several visible lesions. These lesions could be either masses, calcifications, asymmetric densities or architectural distortions. Each is assessed according to a variety of features using CAD systems.

#### 2.6 COMPUTER-AIDED DETECTION (CAD) SYSTEM

CAD is a computer-based process designed to analyze mammographic images for suspicious areas; in effect, it is a "second pair of eyes" for the radiologist.

The U.S. Food and Drug Administration approved CAD for mammography in 1998 and

the Centers for Medicare and Medicaid Services (CMS) increased reimbursement for

CAD in 2002. Measuring the true impact of CAD on the accuracy of mammographic

interpretation has been challenging.

CAD is a relatively young interdisciplinary technology combining elements of artificial

intelligence and digital image processing with radiological image processing.

It is fundamentally based on highly complex pattern recognition. X-ray images are

scanned for suspicious structures. Normally a few thousand images are required to

optimize the algorithm. Digital image data are copied to a CAD server and are prepared

and analyzed in several steps:

1. Preprocessing.

2. Segmentation.

3. Structure/ROI (Region of Interest).

4. Evaluation/classification [10].

2.7 IMAGE PROCESSING

**Image processing** is processing of images using mathematical operations by using any

form of signal processing for which the input is an image, such as a photograph or video

frame; the output of image processing may be either an image or a set of characteristics

or parameters related to the image. Most image-processing techniques involve treating

the image as a two-dimensional signal and applying standard signal-processing

techniques to it.

Image processing usually refers to digital image processing, but optical and analog image

processing also are possible. This article is about general techniques that apply to all of

them. The acquisition of images (producing the input image in the first place) is referred

to as imaging.

2.7.1 DIGITAL IMAGE

Digital image: Discrete samples f[x, y] representing continuous image

f(x,y) Each element of the 2-d array f[x,y] is called a pixel or pel (from "picture

element")

11

#### 2.7.2 DIGITAL IMAGE PROCESSING

Digital image processing is the use of computer algorithms to perform image processing on digital images. As a subcategory or field of digital signal processing, Fundamental steps in image processing:

- 1. Image acquisition: to acquire a digital image
- 2. Image preprocessing: to improve the image in ways that increases the chances for success of the other processes.
- 3. Image segmentation: to partitions an input image into its constituent parts or objects.
- 4. Image representation: to convert the input data to a form suitable for computer processing.
- 5. Image description: to extract features that result in some quantitative information of interest or features that are basic for differentiating one class of objects from another.
- 6. Image recognition: to assign a label to an object based on the information provided by its descriptors.
- 7. Image interpretation: to assign meaning to an ensemble of recognized objects.

#### 2.7.3 Gray Level Coocurrence Matrices

The Gray Level Coocurrence Matrix (GLCM) method is a way of extracting second order statistical texture features. The approach has been used in a number of applications.

A GLCM is a matrix where the number of rows and columns is equal to the number of gray levels G, in the image.

The matrix element  $P(i,j|\Delta x,\Delta y)$  is the relative frequency with which two pixels, separated by a pixel distance  $(\Delta x,\Delta y)$ , occur within a given neighborhood, one with intensity i and the other with intensity j.

One may also say that the matrix element  $p(i, j|d, \theta)$  contains the second order statistical probability values for changes between gray levels i and j at a particular displacement distance d and at a particular angle( $\theta$ ) [11].

#### 2.7.3.1 PROPERTIES OF THE GLCM

The simplest definition of the probability of a given outcome is "the number of times this outcome occurs, divided by the total number of possible outcomes."[12].

#### 2.7.4 HARALICK TEXTURE FEATURES

The proposed algorithms of this study are built on the following features. The Haralick texture features are used for image classification. These features capture information about the patterns that emerge in patterns of texture. The features are calculated by construction a co-occurrence matrix that is traditionally computationally expensive. Once the co-occurrence matrix has been constructed, calculations of the 13 features begin. Some of these features include angular second moment, contrast, correlation, as well as a variety of entropy measures the basis for these features is the gray-level co-occurrence matrix.

Below are described all the features used in the experiment and the meaning of each one in the actual texture analysis case is explained. In all the formulas p(i;j) stands for (i;j)Th entry or value in a normalized GLCM [12].

#### **2.7.4.1 CONTRAST**

Contrast is a local grey level variation in the grey level cooccurrence matrix. It can be thought of as a linear dependency of grey levels of neighboring pixels [12].

$$Contrast = \sum_{i,j=0}^{N-1} P_{i,j} (i-j)^2$$
 (2.1)

#### 2.7.4.2 HOMOGENEITY

Homogeneity measures the uniformity of the non-zero entries in the GLCM. It weights values by the inverse of contrast weight [12].

Homogeneity = 
$$\sum_{i,j=0}^{N-1} \frac{P_{i,j}}{1+(1-j)^2}$$
 (2.2)

The GLCM homogeneity of any texture is high if GLCM concentrates along the diagonal, meaning that there are a lot of pixels with the same or very similar grey level

value. The larger the changes in grey values, the lower the GLCM homogeneity making higher the GLCM contrast. The range of homogeneity is [0, 1].

#### 2.7.4.3 DISSIMILARITY

Dissimilarity is a measure that defines the variation of grey level pairs in an image [12].

$$Dissimilarity = \sum_{i,j=0}^{N-1} P_{i,j} |i-j|$$
 (2.3)

#### **2.7.4.4 ENTROPY**

Entropy in any system represents disorder, where in the case of texture analysis is a measure of its spatial disorder [12].

Entropy = 
$$\sum_{i,j=0}^{N-1} P_{i,j} (-LnP_{i,j})$$
 (2.4)

A completely random distribution would have very high entropy because it represents chaos. Solid tone image would have an entropy value of 0. This feature can be useful to tell us if entropy is bigger for heavy textures or for the smooth textures giving us information about which type of texture can be considered statistically more chaotic [12].

#### **2.7.4.5 ENERGY**

The higher the Energy value, the bigger the homogeneity of the texture. The range of Energy is [0, 1], where Energy is 1 for a constant image [12].

$$Energy = \sum_{i,j=0}^{N-1} P_{i,j}^2$$
 (2.5)

#### **2.8 MATLAB**

The name MATLAB stands for *matrix laboratory*. MATLAB was written originally to provide easy access to matrix software developed by the LINPACK (Linear System Package) and EISPACK (Eigen System Package) projects. Today, MATLAB engines incorporate the LAPACK (Linear Algebra Package) and BLAS (Basic Linear Algebra Subprograms) libraries, constituting the state of the art in software for matrix computation [5].

Typical uses include the following:

- 1. Math and computation.
- 2. Algorithm development.
- 3. Data acquisition.
- 4. Modeling, simulation, and prototyping.
- 5. Data analysis, exploration, and visualization.
- 6. Scientific and engineering graphics.
- 7. Application development, including graphical user interface building.

MATLAB is an interactive system whose basic data element is an array that does not require dimensioning. This allows formulating solutions to many technical computing problems, especially those involving matrix representations, in a fraction of the time it would take to write a program in a scalar non-interactive language such as C or FORTARAN.

**Chapter three** 

Literature review

In this chapter, the evolution of CAD systems and various methodologies used by previous researchers will be overviewed. The ultimate effort for these researchers was to optimize and attain reliable and consistent computerized systems for the augmentation of mammogram interpretation through the application of different feature extraction techniques and procedures.

Incorporation of digital images and image processing within acknowledge based decision aid for radiologists was later developed [13].

## 3.1 COMPUTER –AIDED DETECTION OF BENIGN TUMORS OF FEMAL BREAST

The use of a combination of statistical feature analysis techniques to obtain the best result for the automatic detection of benign tumors in digital mammograms was done by Hamza, A.O *et al.* Where the combination of statistical tools including (mean and median),(mean, median, and standard deviation),(mean, median, and kurtosis),(mean, median, and covariance),(mean, median, and skewedness) and (mean,median,and variance), and concluded that the combination the mean and median were more accurate than the result of the other combinations.}[7].

#### 3.2 COMPUTER-AIDED DETECTION

The introduction of CAD systems provided the opportunity of quick, near real-time performance of analytical computations on digital information that is not readily available to the radiologist until after the cost of film-processing has occurred [14].

A study performed to compare the tumor detection rate with and without use of CAD system resulted in a 2% increase in accuracy using CAD versus without, thus proving that CAD systems are useful additional tools to avoid unnecessary biopsies and to increase accuracy of mammography [15].

#### 3.3 ARTIFICIAL NEURAL NETWORKS

By using different combinations of features, CAD systems with the aid of ANNs (artificial neural networks) were able to classify microcalcifications. Some features and procedures introduced by different researches which finally optimized the detection of micro calcifications by using two ANNs (one for mass detection and one for microcalcifications cluster detection) were used to classify each suspicious region by assigning it a likelihood score for the abnormality under examination [16].

### 3.4DETECTION OF BREAST CANCER CELLS BY USING TEXTURE ANALYSIS

The use of a texture analysis. approach to detect cancer on mammograms was done by Hamza, A.O *et al*. Fifty-five regions of interest (ROIs) containing abnormal breast tissue and 192 ROIs containing normal breast tissue were extracted from digital mammograms obtained from the Mammographic Image Analysis Society database. Haralick texture features derived from spatial grey-level dependence matrix were calculated for each ROI. The importance of each feature in distinguishing abnormal from normal tissues was determined by stepwise linear discriminant analysis. The methodology obtained 92.7% of accuracy for the detection of abnormal tissue (cancer) on digitalized mammograms [17].

#### 3.5 HARALICK TEXTURE FEATURES

A wide variety of methods for describing texture features have been proposed in previous studies. Tuceryan and Jain, divided texture analysis methods into four major categories: statistical, geometrical, model-based and signal processing methods. One commonly applied and referenced method is the co-occurrence method, introduced by Haralick. In this method, the relative frequencies of grey level pairs of pixels separated by a distance d in the direction  $\theta$  combined to form a relative displacement vector (d,  $\theta$ ), which is computed and stored in a matrix, referred to as grey level co-occurrence matrix (GLCM) P. This matrix is used to extract second-order statistical texture features. Haralick suggests 14 features describing the two dimensional probability density function *pij* [18].

#### 3.6 PATTERN RECOGNITION

Pattern recognition methods commonly used for face recognition were applied in order to analyze digital mammograms. The methods are based on novel Classification schemes like the AdaBoost and the support vector machines (SVM). A number of tests have been carried out to evaluate the accuracy of these two algorithms under different circumstances. Results for the AdaBoost classifier method were promising. In the best case the algorithm achieved high accuracy. The SVM based algorithm did not perform as well. In order to achieve a higher accuracy for this method, image features that are better suited for analyzing digital mammograms than the currently used ones should be chosen [19].

The SVM (support vector machines) classification schemes yielded overall maximum accuracy rates, both when the shape type feature was excluded or included in the input vector, higher than the corresponding maximum rates of any other linear or NN alternative. Thus, a representative application of advanced SVM models, compared to

several linear and NN classification schemes, is suggestive to their superiority in classification problems that exhibit high degree of nonlinearity in the training datasets [20].

### 3.7 CONTRAST-LIMITED ADAPTIVE HISTOGRAM EQUALIZATION

A study was performed to determine whether contrast-limited adaptive histogram equalization (CLAHE) or histogram-based intensity windowing (HIW) improves the detection of simulated masses in dense mammograms. The success in detecting simulated masses on mammograms with dense backgrounds depended on the parameter settings of the algorithms used. The best HIW setting performed better than the best fixed-intensity window setting and better than no processing.

Performance with the best CLAHE settings was no different from that with no processing. In the HIW experiment, there were no significant differences in observer performance between processing conditions for radiologists and non-radiologists [21].

# Chapter Four Materials and Methods

4.1 STAGE I: THE DIFFERENCE BETWEEN

RADIOLOGIST DIAGNOSIS

The first phase of this study involved choosing a sample of 20 digital mammograms

containing one or two benign tumors and presenting them to 3 different radiologists for

interpretation.

4.1.1 SAMPLE SELECTION

Digital mammograms were obtained from the mini-MIAS (Mammographic Image

Analysis Society) database [22].

The mammograms by popular request, the original MIAS database (digitised at 50

micron pixel edge) has been reduced to 200micron pixel edge and clipped/padded so that

every image is 1024 x 1024 pixels.

The follow list gives the films in the MIAS database and provides appropriate

details as follows:

First column: MIAS database reference number.

**Second column:** character of background tissue:

a. F Fatty

b. G Fatty-glandular

c. D Dense-glandular

**Third column:** Class of abnormality present:

a. CALC Calcification

b. CIRC Well-defined/circumscribed masses

c. SPIC Spiculated masses

d. MISC Other, ill-defined masses

e. ARCH Architectural distortion

f. ASYM Asymmetry

g. NORM Normal

Fourth column: severity of abnormality:

a. B Benign

b. M Malignant

**Fifth, Sixth columns:** X, Y image-coordinates of centre of abnormality.

**Seventh column:** Approximate radius (in pixel) of a circle enclosing the abnormality.

21

All of the chosen mammograms have been diagnosed by experts of radiology. They all contained the following features:

- 1. Benign.
- 2. Circular shape.
- 3. PGM format.
- 4. 1024 x 1024 sizes.
- 5. 8-bit color.
- 6. 1 MB pixels.

Each mammogram contains either one or two benign tumors of variable sizes and different tissue type (fatty, dense or fatty glandular tissue).

#### 4.1.2 VISUAL INSPECTION OF MAMMOGRAMS

Three radiologists (Radiologists A, B and C) were chosen to visually inspect the sample.

The radiologists were asked to specify the region of tumor in each image by drawing a circle around it using the Microsoft Paint application.

#### 4.2 STAGE II: IMAGE ANALYSIS

This stage involves developing an image processing algorithm that can automatically detect benign tumors in digital mammograms.

#### 4.2.1 ROI (REGON OF INTEREST) SELECTION

In each mammogram image two (2) frames were selected, one represents normal tissue and other represents abnormal tissue.

#### 4.2.2 ALGORITHM DEVELOPMENT

The following haralick feature analysis techniques were tested in order to automatically detect benign tumors:

- a. Contrast.
- b. Energy.
- c. Homogeneity.

The above features were tested in order to determine the best method of benign tumor detection. This was done by developing a MATLAB code that divides the input image into small frames, each frame having a size of 51 x 51 pixels.

The developed code (see **Appendix I**) reads the input image that contains the tumor. It then moves frame by frame, each time calculating each of the haralick features.

The following figure, Figure (3.1) shows the flowchart used for the proposed algorithm that incorporates the **contrast**, **energy** and **homogeneity** haralick features.

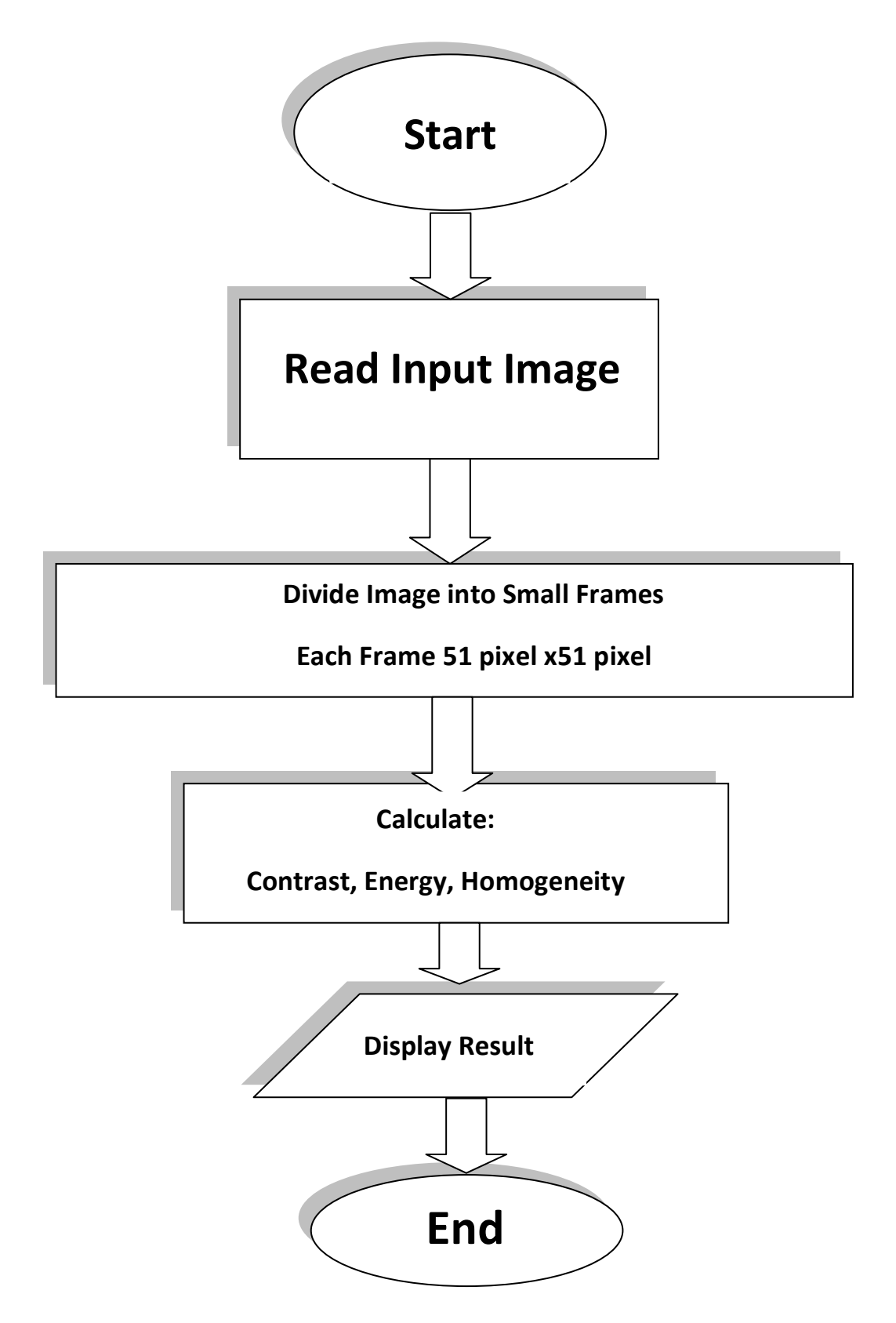
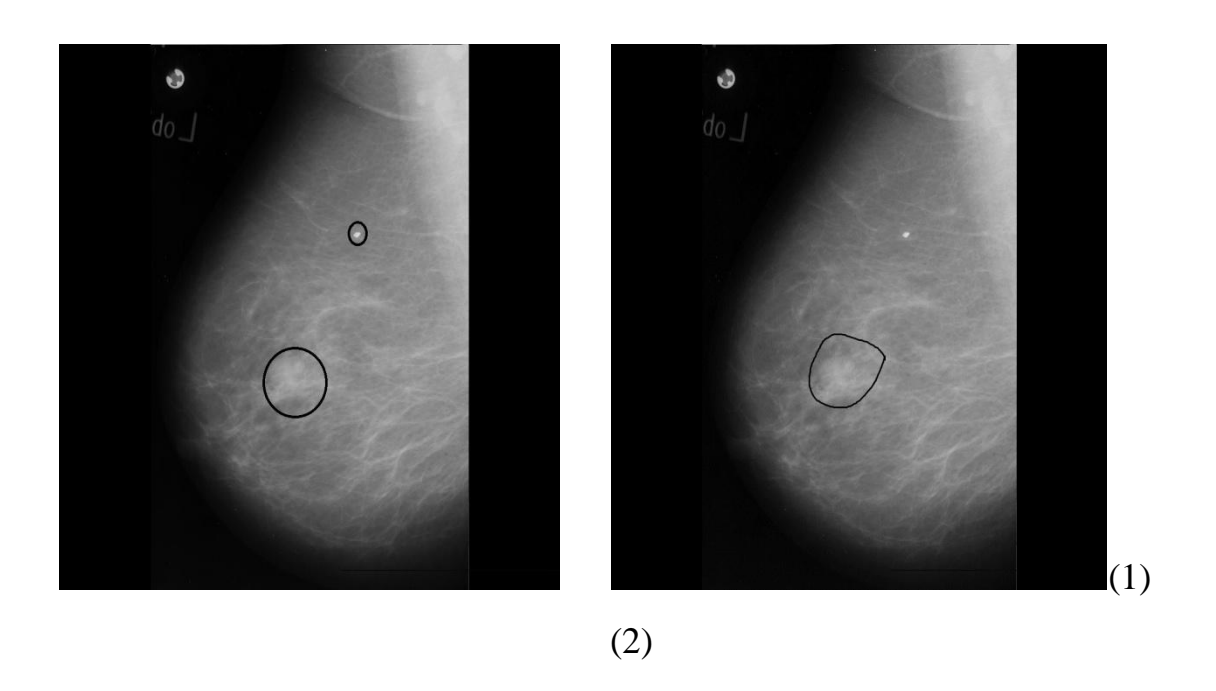


Figure 4.1shows the Algorithm flowchart for code using mean and median.

Chapter Five Results and Discussion

#### 5.1. RADIOLOGIST VARIABILITY

The following figures show the variability amongst radiologists A, B and C in interpreting the tumor in each mammogram.



------

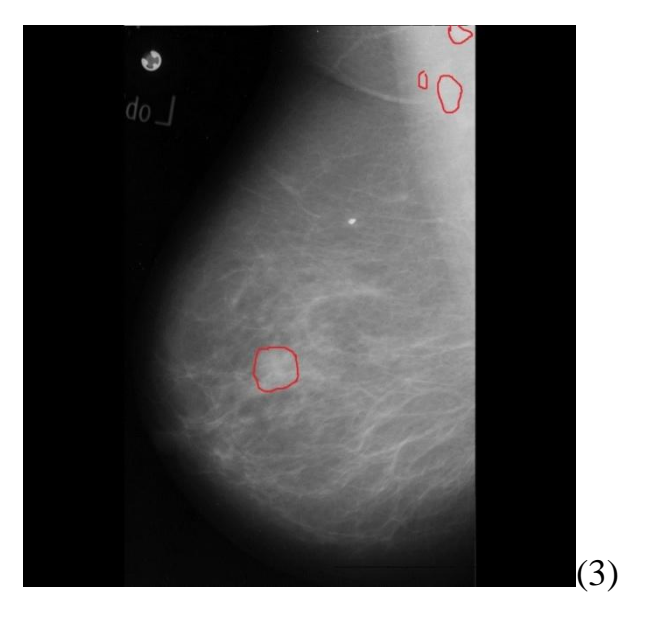


Figure 5.1 shows the img1 as diagnosed by (1) radiologist A, (2) radiologist B, (3) radiologist C The radiologist diagnosis is marked by the circles.

It is clear from the above figures that the radiologists are not consistent in determining the number of the tumor.

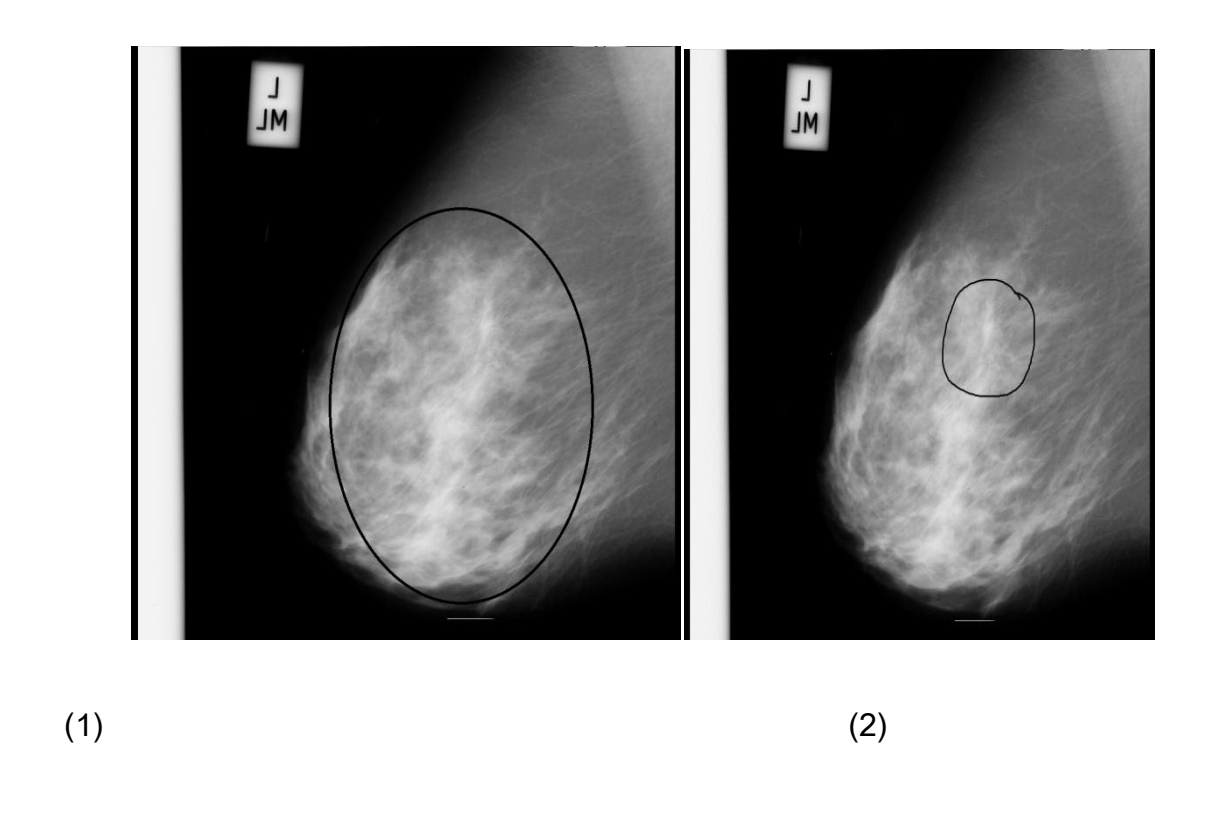




Figure 5.2 shows the img2 as diagnosed by (1) radiologist A, (2) radiologist B, (3) radiologist C The radiologist diagnosis is marked by the circles.

It is clear from the above figures that the radiologists are not consistent in determining the size of the tumor.

A comparison was made in tables (5.1 , 5.2 , 5.3 , 5.4 , 5.5 , 5.6 , 5.7 , 5.8 , 5.9 , 5.10 , 5.11 , 5.12 , 5.13 , 5.14 , 5.15 , 5.16 , 5.17 , 5.18 , 5.19 , 5.20 ) below between normal frames and abnormal frames using Haralick Texture feature (Contrast, Energy and Homogeneity) with  $\theta$ =0 (Horizontal) and d=1 with matlab program.

Table 5.1 comparison between normal frame and abnormal frame

	No.	contrast tumor	contrast normal	energy tumor	energy normal	homo tumor	homo normal
	1	26.3153	35.8196	0.2255	0.1257	0.5128	0.5374
	2	20.4439	26.0141	0.1609	0.3054	0.6389	0.5436
	3	27.142	11.8212	0.1353	0.2564	0.6376	0.6797
	4	31.6157	10.1024	0.1242	0.2205	0.5912	0.5507
	5	15.8525	36.5725	0.166	0.1408	0.6338	0.5533
	6	25.5373	22.0306	0.3158	0.1525	0.5412	0.5805
	7	23.6298	13.4275	0.2064	0.339	0.5291	0.6462
mdb001.pgm	8	22.2478	8.1443	0.0906	0.2724	0.5972	0.5809
	9	13.4478		0.1831		0.6241	
	10	28.1098		0.2557		0.5665	
	11	22.858		0.321		0.6246	
	12	19.8463		0.158		0.5888	
	13	22.5506		0.2764		0.6318	
	14	27.4635		0.2124		0.5118	
	15	10.811		0.2165		0.5712	
	16	23.6894		0.2126		0.6265	
	total	361.5607	163.9322	3.2604	1.8127	9.4271	4.6723
	average	22.59754375	20.491525	0.203775	0.2265875	0.58919375	0.5840375

Table 5.2 comparison between normal frame and abnormal frame

	No.	contrast tumor	contrast normal	energy tumor	energy normal	homo tumor	homo normal
	1	39.9627	34.2941	0.1319	0.3047	0.588	0.5758
	2	29.0867	28.8706	0.13	0.2541	0.5805	0.5554
	3	19.0749	31.5608	0.1593	0.2761	0.647	0.5085
mdb005.pgm	4	28.2737	28.5976	0.097	0.2546	0.6012	0.5728
	5	24.2216	34.742	0.1097	0.2577	0.5751	0.4652
	6	32.0878	31.7749	0.0922	0.2641	0.5697	0.5039
	total	172.7074	189.84	0.7201	1.6113	3.5615	3.1816
	average	28.78456667	31.64	0.12001667	0.26855	0.593583333	0.530266667

Table 5.3 comparison between normal frame and abnormal frame

	No.	contrast tumor	contrast normal	energy tumor	energy normal	homo tumor	homo normal
	1	33.3663	26.411	0.1683	0.2359	0.6016	0.5991
	2	24.2275	12.1443	0.1223	0.2195	0.5765	0.5762
	3	36.0659	28.6965	0.2068	0.2732	0.5862	0.5566
mdb010.pgm	4	31.8039	25.1859	0.2491	0.2921	0.3606	0.6035
	total	125.4636	92.4377	0.7465	1.0207	2.1249	2.3354
	average	31.3659	23.109425	0.186625	0.255175	0.531225	0.58385

Table 5.4 comparison between normal frame and abnormal frame

	No.	contrast tumor	contrast normal	energy tumor	energy normal	homo tumor	homo normal
	1	29.5125	35.2078	0.048	0.2139	0.5865	0.6005
	2	37.4102	31.4682	0.218	0.194	0.5038	0.5922
	3	18.0424	48.6055	0.1223	0.2311	0.6407	0.5055
	4	30.2122	32.9757	0.0846	0.2006	0.6025	0.6083
mdb017pgm	5	28.6745	20.9349	0.2393	0.1406	0.5432	0.6035
	6	33.2314	37.9106	0.1342	0.146	0.5531	0.5542
	7	25.7235	22.9243	0.1139	0.053	0.6423	0.6442
	8	27.3365	20.4659	0.2403	0.1484	0.5559	0.6488
	9	34.7482	33.5247	0.2171	0.1495	0.5807	0.5855
	total	264.8914	284.0176	1.4177	1.4771	5.2087	5.3427
	average	29.43237778	31.55751111	0.15752222	0.164122222	0.578744444	0.593633333

Table 5.5 comparison between normal frame and abnormal frame

	No.	contrast tumor	contrast normal	energy tumor	energy normal	homo tumor	homo normal
	1	42.7114	32.6392	0.3288	0.2455	0.6334	0.5268
	2	51.051	40.0271	0.1377	0.3058	0.5904	0.5335
	3	24.44	71.3063	0.1181	0.2205	0.6319	0.5371
	4	25.8204	43.7176	0.1409	0.3637	0.5717	0.6448
	5	36.5055	62.5765	0.1473	0.2865	0.6069	0.5493
	6	38.1302	41.7922	0.151	0.2464	0.5087	0.6028
mdb025.pgm	7	42.2086	29.431	0.183	0.2447	0.422	0.5831
	8	27.2125	57.6282	0.1585	0.3026	0.6206	0.6252
	9	43.5859	59.6757	0.1979	0.222	0.6482	0.5618
	10	28.0114	50.8416	0.112	0.3504	0.6232	0.6252
	11	21.8149	39.4427	0.1224	0.1739	0.5767	0.5934
	12	14.5114	38.8333	0.2268	0.2998	0.5916	0.5815
	total	396.0032	567.9114	2.0244	3.2618	7.0253	6.9645
	average	33.00026667	47.32595	0.1687	0.271816667	0.585441667	0.580375

Table 5.6 comparison between normal frame and abnormal frame

	No.	contrast tumor	contrast normal	energy tumor	energy normal	homo tumor	homo normal
	1	23.4086	22.3639	0.1165	0.1183	0.6056	0.5732
	2	34.2557	52.671	0.2277	0.1979	0.6205	0.539
	3	18.1412	33.918	0.1548	0.2632	0.5651	0.5797
	4	35.9906	25.309	0.1869	0.1325	0.5386	0.5512
mdb063.pgm	5	22.8157	73.4808	0.1403	0.2411	0.6071	0.5446
	6	33.1231	27.3588	0.1403	0.2801	0.5845	0.6077
	7	37.4416	33.6729	0.2085	0.1133	0.5719	0.5816
	8	19.1169	37.4482	0.1597	0.2695	0.6083	0.6099
	9	27.6392	22.4627	0.1081	0.2703	0.5823	0.5399
	total	251.9326	328.6853	1.4428	1.8862	5.2839	5.1268
	average	27.99251111	36.52058889	0.16031111	0.209577778	0.5871	0.569644444

Table 5.7 comparison between normal frame and abnormal frame

	No.	contrast tumor	contrast normal	energy tumor	energy normal	homo tumor	homo normal
	1	34.971	53.6027	0.1545	0.1951	0.6029	0.5814
	2	27.858	36.8733	0.1243	0.1233	0.6153	0.5901
	3	10.7231	39.6616	0.2273	0.1398	0.6265	0.5882
mdb069.pgm	4	32.4627	18.0329	0.1101	0.1519	0.6091	0.6445
	5	19.5055	21.0761	0.1868	0.2	0.6227	0.6097
	6	14.2651	27.0008	0.1925	0.1472	0.5855	0.6173
	total	139.7854	196.2474	0.9955	0.9573	3.662	3.6312
	average	23.29756667	32.7079	0.16591667	0.15955	0.610333333	0.6052

Table 5.8 comparison between normal frame and abnormal frame

	No.	contrast tumor	contrast norma	lenergy tumoi	energy normal	homo tumor	homo norma
	1	21.0702	16.8212	0.1121	0.1703	0.5729	0.5982
	2	43.4255	36.4322	0.1423	0.2136	0.5833	0.6151
	3	28.1573	39.0133	0.0833	0.2778	0.5478	0.6369
	4	30.9522	34.5592	0.0997	0.3248	0.5525	0.6073
	5	18.1302	22.7792	0.1386	0.2213	0.5732	0.6252
	6	11.0557	26.7357	0.2126	0.2547	0.6113	0.5252
	7	33.9396	33.0431	0.1127	0.2221	0.5924	0.6232
	8	23.6216	71.7894	0.0761	0.2616	0.5757	0.5398
	9	9.4243	25.0631	0.267	0.2877	0.664	0.5823
	10	14.9082	35.3392	0.2559	0.2296	0.5999	0.5989
	11	26.0157	32.8671	0.1589	0.2827	0.6394	0.6701
	12	19.7271	23.5573	0.2155	0.2301	0.5886	0.5931
	13	37.8443	52.6502	0.0797	0.2904	0.5519	0.5812
	14	16.6478	65.9859	0.1606	0.2648	0.5628	0.5726
mdb081.pgm	15	24.5522	70.2706	0.3904	0.2713	0.598	0.5676
	16	18.4408	75.3051	0.2079	0.2395	0.5323	0.6222
	17	28.6329	41.2008	0.1357	0.3055	0.5878	0.6017
	18	25.4102	35.1992	0.147	0.2439	0.548	0.5625
	19	33.7027	33.3702	0.0977	0.1676	0.5481	0.6132
	20	14.3027	54.7725	0.182	0.2649	0.5693	0.6224
	21	24.7592	55.0761	0.1753	0.311	0.4539	0.6224
	22	21.1827	50.5294	0.2338	0.2104	0.4997	0.5958
	23	22.6306	63.9682	0.2036	0.1909	0.6001	0.514
	24	33.4745	45.1243	0.1461	0.1518	0.5633	0.5876
	25	21.622	25.6667	0.1237	0.0888	0.63	0.5976
	26	28.3373	30.7141	0.1201	0.1124	0.5835	0.5987
	27	32.2745	27.2541	0.1598	0.1345	0.5475	0.5036
	28	25.3176	21.5176	0.1659	0.1579	0.5489	0.5402
	29	24.5616	18.4675	0.0968	0.155	0.6121	0.6137
	30	22.2275	25.4322	0.1259	0.1033	0.6218	0.5984
		700 0407	1100 E017	4.0007	0.0400	17.26	17 7007
	total average	736.3487 24.54495667	1190.5047 39.68349	4.8267 0.16089	6.6402 0.22134	0.575333333	17.7307 0.591023333

Table 5.9 comparison between normal frame and abnormal frame

	No.	contrast tumor	contrast normal	energy tumor	energy normal	homo tumor	homo normal
	1	13.8478	22.5992	0.1702	0.2741	0.6259	0.5953
	2	18.0549	25.7255	0.1864	0.3348	0.6328	0.5475
	3	30.72	19.8588	0.1332	0.405	0.5871	0.6397
mdb083.pgm	4	29.7427	24.0188	0.0875	0.3054	0.6317	0.5553
	5	17.3537	22.1427	0.087	0.3044	0.6351	0.5762
	6	22.038	24.7216	0.0722	0.3922	0.5909	0.5935
	total	131.7571	139.0666	0.7365	2.0159	3.7035	3.5075
	average	21.95951667	23.17776667	0.12275	0.335983333	0.61725	0.584583333

Table 5.10 comparison between normal frame and abnormal frame

	No.	contrast tumor	contrast normal	energy tumo	r energy normal	homo tumor	homo normal
	1	30.6694	60.4643	0.1735	0.2046	0.5916	0.5017
	2	23.6769	26.7216	0.1144	0.1044	0.5874	0.5379
mdb104.pgm	3	25.8745	23.2737	0.129	0.1591	0.4886	0.5171
	4	35.7078	42.3506	0.1624	0.339	0.5659	0.5805
	5	12.9286	23.1655	0.1921	0.1386	0.5422	0.543
	6	21.531	20.1718	0.1415	0.1206	0.5813	0.5878
	total	150.3882	196.1475	0.9129	1.0663	3.357	3.268
	average	25.0647	32.69125	0.15215	0.177716667	0.5595	0.544666667

Table 5.11 comparison between normal frame and abnormal frame

	No.	contrast tumor	contrast normal	energy tumor	energy normal	homo tumor	homo normal
	1	13.9373	12.5427	0.1943	0.3997	0.5855	0.6579
	2	36.16	8.2698	0.1002	0.295	0.5231	0.5953
	3	20.9804	24.8282	0.1561	0.3164	0.6019	0.5665
	4	12.4549	24.1992	0.1288	0.2371	0.5757	0.5867
	5	28.4455	7.6486	0.2203	0.2709	0.6021	0.6024
mdb132.pgm	6	24.2204	7.8682	0.1594	0.2751	0.5289	0.5633
	7	29.8298	13.189	0.2464	0.3713	0.5788	0.6603
	8	42.0635	17.8259	0.1903	0.4234	0.6275	0.6535
	total	208.0918	116.3716	1.3958	2.5889	4.6235	4.8859
	average	26.011475	14.54645	0.174475	0.3236125	0.5779375	0.6107375

Table 5.12 comparison between normal frame and abnormal frame

	No.	contrast tumor	contrast normal	energy tumor	energy normal	homo tumor	homo normal
	1	24.7749	30.1427	0.14	0.2536	0.5997	0.5948
mdb142.pgm	2	33.4494	26.1443	0.2141	0.2635	0.6066	0.6002
	total	58.2243	56.287	0.3541	0.5171	1.2063	1.195
	average	29.11215	28.1435	0.17705	0.25855	0.60315	0.5975

Table 5.13 comparison between normal frame and abnormal frame

	No.	contrast tumor	contrast normal	energy tumor	energy normal	homo tumor	homo normal
mdb144.pgm	1	22.9522	24.1631	0.1702	0.1046	0.5825	0.5851
	total	22.9522	24.1631	0.1702	0.1046	0.5825	0.5851
	average	22.9522	24.1631	0.1702	0.1046	0.5825	0.5851

Table 5.14 comparison between normal frame and abnormal frame

	No.	contrast tumor	contrast normal	energy tumor	energy normal	homo tumor	homo normal
	1	12.5671	22.24	0.4398	0.2633	0.7171	0.6029
	2	17.3733	30.0878	0.1002	0.26	0.5434	0.565
	3	22.7471	29.8196	0.0832	0.2807	0.6214	0.5463
mdb150.pgm	4	23.7282	34.0086	0.0666	0.2511	0.6008	0.4876
	5	22.8369	40.2996	0.1212	0.2299	0.5722	0.4682
	6	36.2694	18.1337	0.1097	0.3102	0.5979	0.6577
	7	24.6086	17.9557	0.1706	0.3686	0.565	0.6586
	8	32.6761	25.2408	0.2222	0.2954	0.6251	0.6187
	9	26.9973	33.9082	0.1631	0.2601	0.592	0.4788
	10	25.9812	37.1396	0.0669	0.2642	0.6128	0.4293
	11	29.7906	18.3827	0.1063	0.181	0.5739	0.5745
	12	26.1992	23.8475	0.1769	0.2366	0.5971	0.5856
	13	29.3302	24.6408	0.2287	0.3422	0.6588	0.6194
	14	28.538	24.2784	0.1449	0.314	0.6243	0.6232
	15	19.4825	34.8922	0.1602	0.2348	0.59	0.537
	total	379.1257	414.8752	2.3605	4.0921	9.0918	8.4528
	average	25.27504667	27.65834667	0.15736667	0.272806667	0.60612	0.56352

Table 5.15 comparison between normal frame and abnormal frame

	No.	contrast tumor	contrast normal	energy tumor	energy normal	homo tumor	homo normal
	1	41.2486	34.778	0.2688	0.2895	0.3616	0.4725
	2	21.5592	22.6588	0.3043	0.4627	0.5735	0.6834
mdb152.pgm	3	11.9718	20.6588	0.2168	0.5487	0.5825	0.7411
	4	34.1961	30.5725	0.2735	0.2823	0.4592	0.5335
	5	10.2965	33.8855	0.2323	0.2524	0.5906	0.4791
	6	8.6275	23.2471	0.4451	0.4523	0.6757	0.6673
	total	127.8997	165.8007	1.7408	2.2879	3.2431	3.5769
	average	21.31661667	27.63345	0.29013333	0.381316667	0.540516667	0.59615

Table 5.16 comparison between normal frame and abnormal frame

	No.	contrast tumor	contrast normal	energy tumor	energy normal	homo tumor	homo normal
	1	8.6298	24.3765	0.306	0.3636	0.6584	0.6094
	2	14.2482	9.8902	0.2756	0.4552	0.6389	0.7156
mdb190.pgm	3	7.9937	22.7169	0.3478	0.3018	0.5788	0.667
	4	10.0651	11.3992	0.3915	0.3081	0.7148	0.6081
	total	40.9368	68.3828	1.3209	1.4287	2.5909	2.6001
	average	10.2342	17.0957	0.330225	0.357175	0.647725	0.650025

Table 5.17 comparison between normal frame and abnormal frame

	No.	contrast tumor	contrast normal	energy tumor	energy normal	homo tumor	homo normal
	1	27.1275	10.2525	0.0536	0.27	0.5973	0.6259
	2	24.6933	10.102	0.1274	0.418	0.6094	0.6903
mdb195.pgm	3	21.8929	11.8965	0.1019	0.4233	0.629	0.6622
	4	29.6925	25.3482	0.115	0.2618	0.5994	0.609
	5	23.8776	23.2722	0.0931	0.24	0.6271	0.5381
	6	28.9569	49.5824	0.1278	0.1509	0.5942	0.5911
	total	156.2407	130.4538	0.6188	1.764	3.6564	3.7166
	average	26.04011667	21.7423	0.10313333	0.294	0.6094	0.619433333

Table 5.18 comparison between normal frame and abnormal frame

	No.	contrast tumor	contrast normal	energy tumor	energy normal	homo tumor	homo normal
	1	12.5929	58.9353	0.2815	0.3054	0.5819	0.597
	2	25.7725	60.622	0.1253	0.2338	0.5868	0.5573
	3	29.729	20.6698	0.0695	0.1364	0.5719	0.5471
	4	22.1365	85.8804	0.1657	0.2663	0.5573	0.4909
	5	33.8682	63.2976	0.1386	0.2374	0.5577	0.5659
	6	20.1627	26.3522	0.1242	0.174	0.5821	0.5336
	7	34.3231	76.76	0.1659	0.2815	0.5531	0.5106
mdb198.pgm	8	12.2667	37.0729	0.3219	0.3225	0.6005	0.5856
	9	24.0424	46.2357	0.1461	0.1607	0.6291	0.599
	10	33.0102		0.1488		0.5941	
	11	29.1718		0.1648		0.5401	
	12	43.8227		0.1918		0.5204	
	13	39.1247		0.2344		0.5834	
	14	34.6557		0.2087		0.6021	
	15	35.1671		0.2856		0.5761	
	total	429.8462	475.8259	2.7728	2.118	8.6366	4.987
	average	28.65641333	52.86954444	0.18485333	0.235333333	0.575773333	0.554111111

Table 5.19 comparison between normal frame and abnormal frame

	No.	contrast tumor	contrast normal	energy tumor	energy normal	homo tumor	homo normal
	1	31.0631	51.3455	0.0837	0.1845	0.6098	0.6094
	2	15.9341	16.8588	0.1899	0.187	0.6075	0.5958
mdb290.pgm	3	26.6945	23.5153	0.1015	0.1057	0.5959	0.5826
	4	25.6533	36.891	0.1417	0.1525	0.6119	0.5722
	5		31.9282		0.077		0.5872
	6		31.1067		0.1147		0.5762
	total	99.345	191.6455	0.5168	0.8214	2.4251	3.5234
	average	24.83625	31.94091667	0.1292	0.1369	0.606275	0.587233333

Table 5.20 comparison between normal frame and abnormal frame

	No.	contrast tumor	contrast normal	energy tumor	energy normal	homo tumor	homo normal
	1	31.0631	51.3455	0.0837	0.1845	0.6098	0.6094
	2	15.9341	16.8588	0.1899	0.187	0.6075	0.5958
mdb290.pgm	3	26.6945	23.5153	0.1015	0.1057	0.5959	0.5826
	4	25.6533	36.891	0.1417	0.1525	0.6119	0.5722
	5		31.9282		0.077		0.5872
	6		31.1067		0.1147		0.5762
	total	99.345	191.6455	0.5168	0.8214	2.4251	3.5234
	average	24.83625	31.94091667	0.1292	0.1369	0.606275	0.587233333

Table 5.21 contrast average

No.	picture	contrast tumor	contrast normal	diffrence
1	mdb001.pgm	22.59754375	20.491525	-2.10601875
2	mdb005.pgm	28.78456667	31.64	2.855433333
3	mdb010.pgm	31.3659	23.109425	-8.256475
4	mdb017pgm	29.43237778	31.55751111	2.125133333
5	mdb025.pgm	33.00026667	47.32595	14.32568333
6	mdb063.pgm	27.99251111	36.52058889	8.528077778
7	mdb069.pgm	23.29756667	32.7079	9.410333333
8	mdb081.pgm	24.54495667	39.68349	15.13853333
9	mdb083.pgm	21.95951667	23.17776667	1.21825
10	mdb104.pgm	25.0647	32.69125	7.62655
11	mdb132.pgm	26.011475	14.54645	-11.465025
12	mdb142.pgm	29.11215	28.1435	-0.96865
13	mdb144.pgm	22.9522	24.1631	1.2109
14	mdb150.pgm	25.27504667	27.65834667	2.3833
15	mdb152.pgm	21.31661667	27.63345	6.316833333
16	mdb190.pgm	10.2342	17.0957	6.8615
17	mdb195.pgm	26.04011667	21.7423	-4.297816667
18	mdb198.pgm	28.65641333	52.86954444	24.21313111
19	mdb248.pgm	28.61118333	21.18065	-7.430533333
20	mdb290.pgm	24.83625	31.94091667	7.104666667

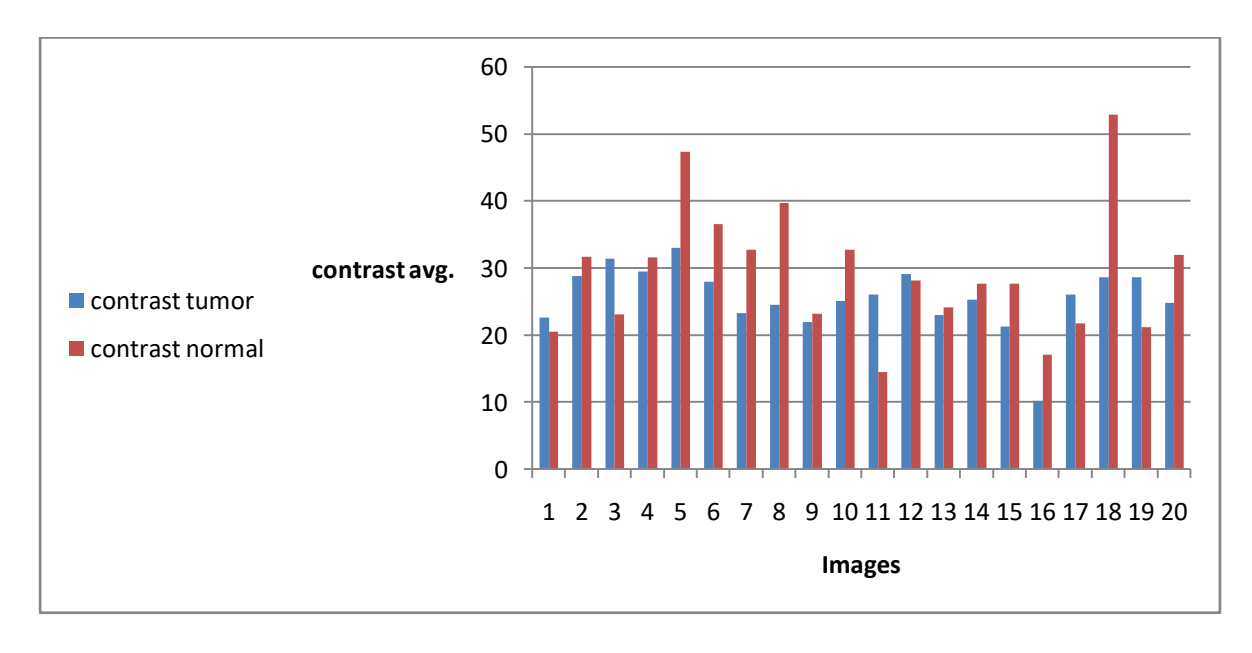


Figure 5.3 shows the contrast average calculated by MATLAB code

Table 5.22 Energy average

No.	picture	energy tumor	energy normal	diffrence
1	mdb001.pgm	0.203775	0.2265875	0.0228125
2	mdb005.pgm	0.120016667	0.26855	0.148533333
3	mdb010.pgm	0.186625	0.255175	0.06855
4	mdb017pgm	0.157522222	0.164122222	0.0066
5	mdb025.pgm	0.1687	0.271816667	0.103116667
6	mdb063.pgm	0.160311111	0.209577778	0.049266667
7	mdb069.pgm	0.165916667	0.15955	-0.006366667
8	mdb081.pgm	0.16089	0.22134	0.06045
9	mdb083.pgm	0.12275	0.335983333	0.213233333
10	mdb104.pgm	0.15215	0.177716667	0.025566667
11	mdb132.pgm	0.174475	0.3236125	0.1491375
12	mdb142.pgm	0.17705	0.25855	0.0815
13	mdb144.pgm	0.1702	0.1046	-0.0656
14	mdb150.pgm	0.157366667	0.272806667	0.11544
15	mdb152.pgm	0.290133333	0.381316667	0.091183333
16	mdb190.pgm	0.330225	0.357175	0.02695
17	mdb195.pgm	0.103133333	0.294	0.190866667
18	mdb198.pgm	0.184853333	0.235333333	0.05048
19	mdb248.pgm	0.133316667	0.244316667	0.111
20	mdb290.pgm	0.1292	0.1369	0.0077

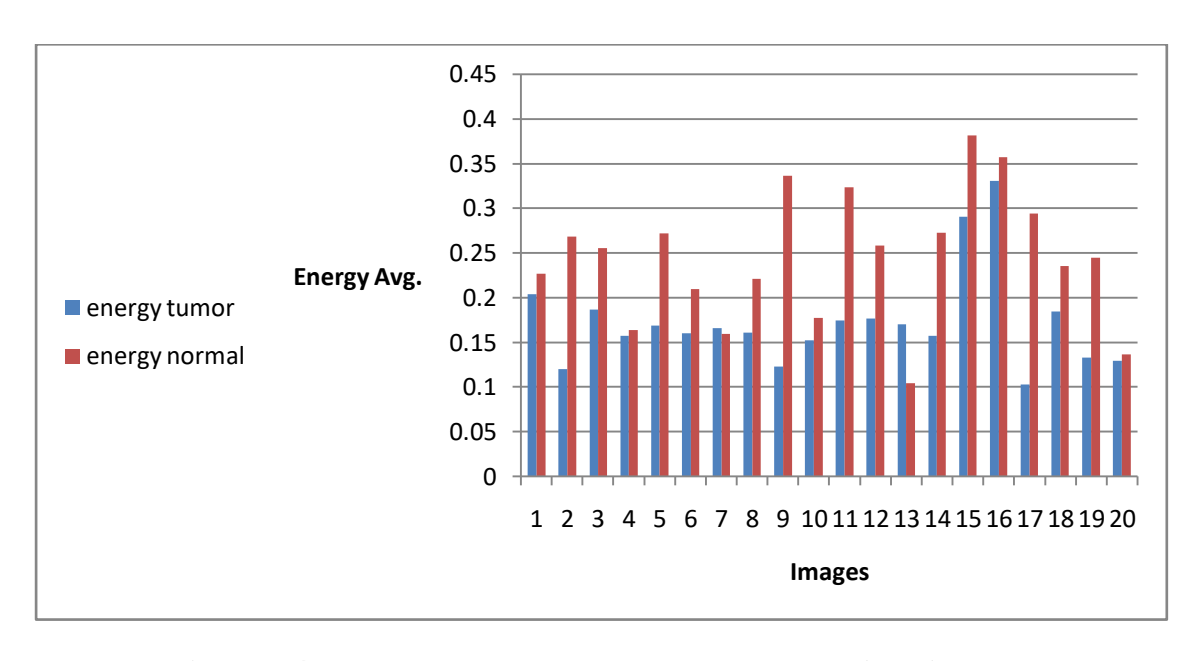


Figure 5.4 shows energy average calculated by MATLAB code

#### Images below represent the output of the energy average (max and min)

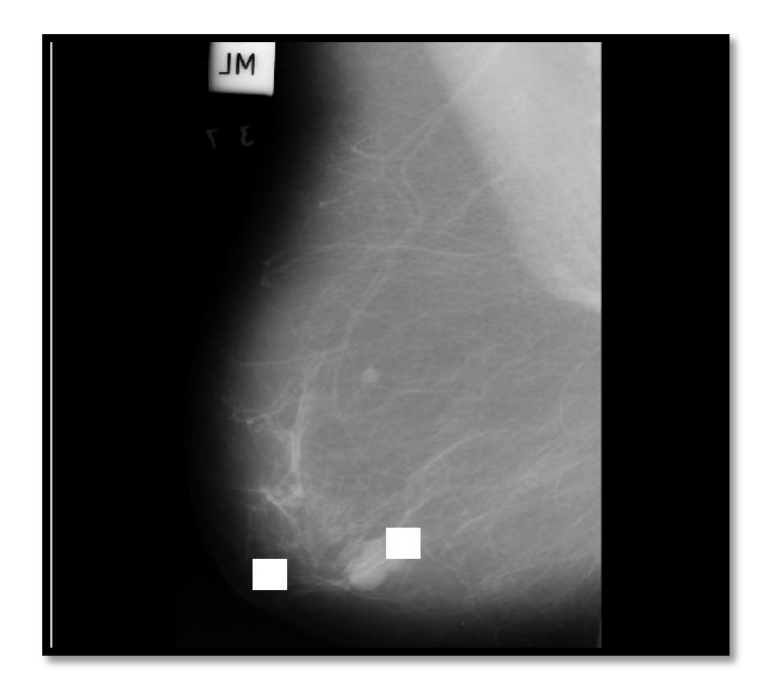


Figure 5.5 shows the image mdb005.pgm

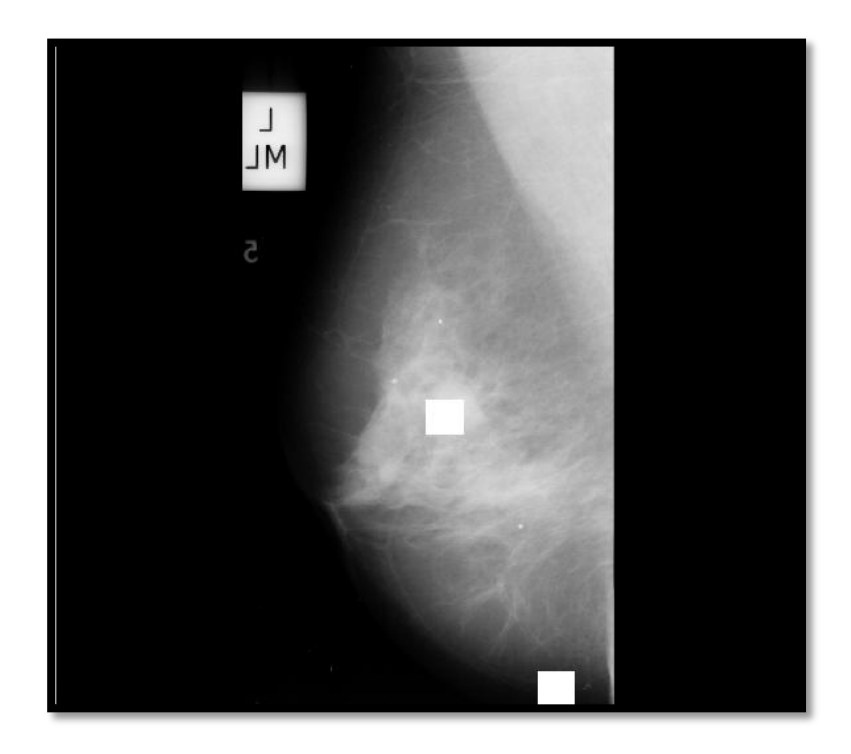


Figure 5.6 shows the image 063.pgm

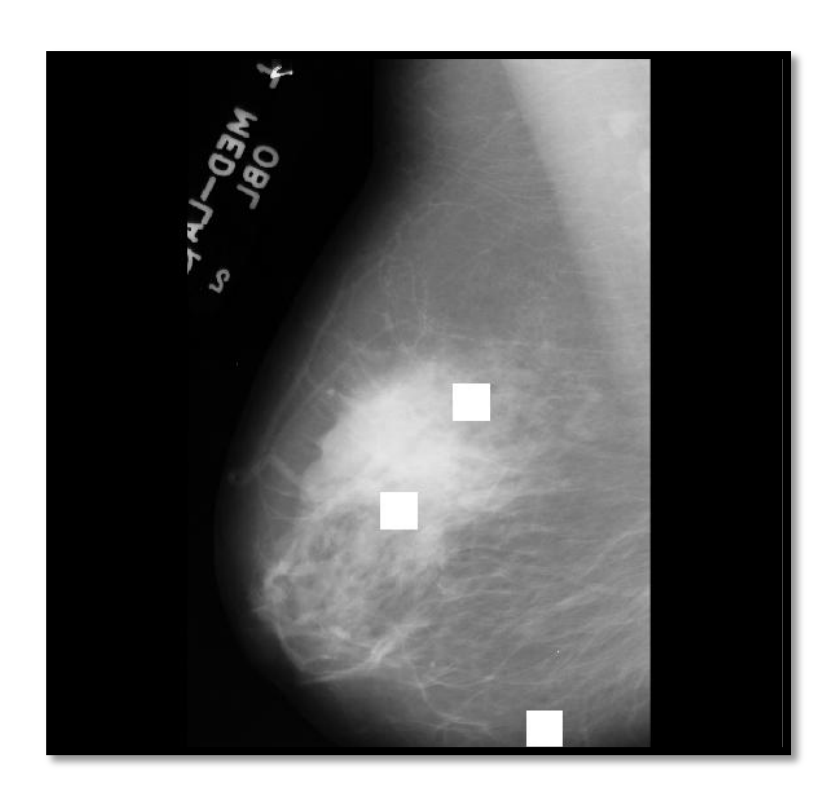


Figure 5.7 shows the image mad081.pgm

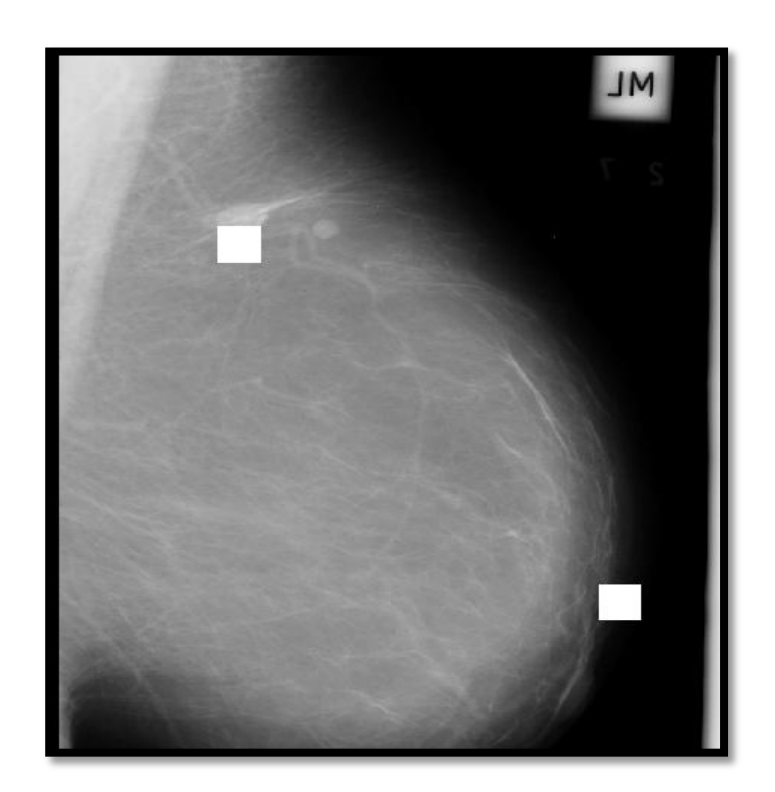


Figure 5.8 shows the image132.pgm

**Table 5.23 Homogeneity average** 

No.	picture	homo tumor	homo normal	diffrence
1	mdb001.pgm	0.58919375	0.5840375	0.00515625
2	mdb005.pgm	0.593583333	0.530266667	0.063316667
3	mdb010.pgm	0.531225	0.58385	-0.052625
4	mdb017pgm	0.578744444	0.593633333	-0.014888889
5	mdb025.pgm	0.585441667	0.580375	0.005066667
6	mdb063.pgm	0.5871	0.569644444	0.017455556
7	mdb069.pgm	0.610333333	0.6052	0.005133333
8	mdb081.pgm	0.575333333	0.591023333	-0.01569
9	mdb083.pgm	0.61725	0.584583333	0.032666667
10	mdb104.pgm	0.5595	0.544666667	0.014833333
11	mdb132.pgm	0.5779375	0.6107375	-0.0328
12	mdb142.pgm	0.60315	0.5975	0.00565
13	mdb144.pgm	0.5825	0.5851	-0.0026
14	mdb150.pgm	0.60612	0.56352	0.0426
15	mdb152.pgm	0.540516667	0.59615	-0.055633333
16	mdb190.pgm	0.647725	0.650025	-0.0023
17	mdb195.pgm	0.6094	0.619433333	-0.010033333
18	mdb198.pgm	0.575773333	0.554111111	0.021662222
19	mdb248.pgm	0.598616667	0.564783333	0.033833333
20	mdb290.pgm	0.606275	0.587233333	0.019041667

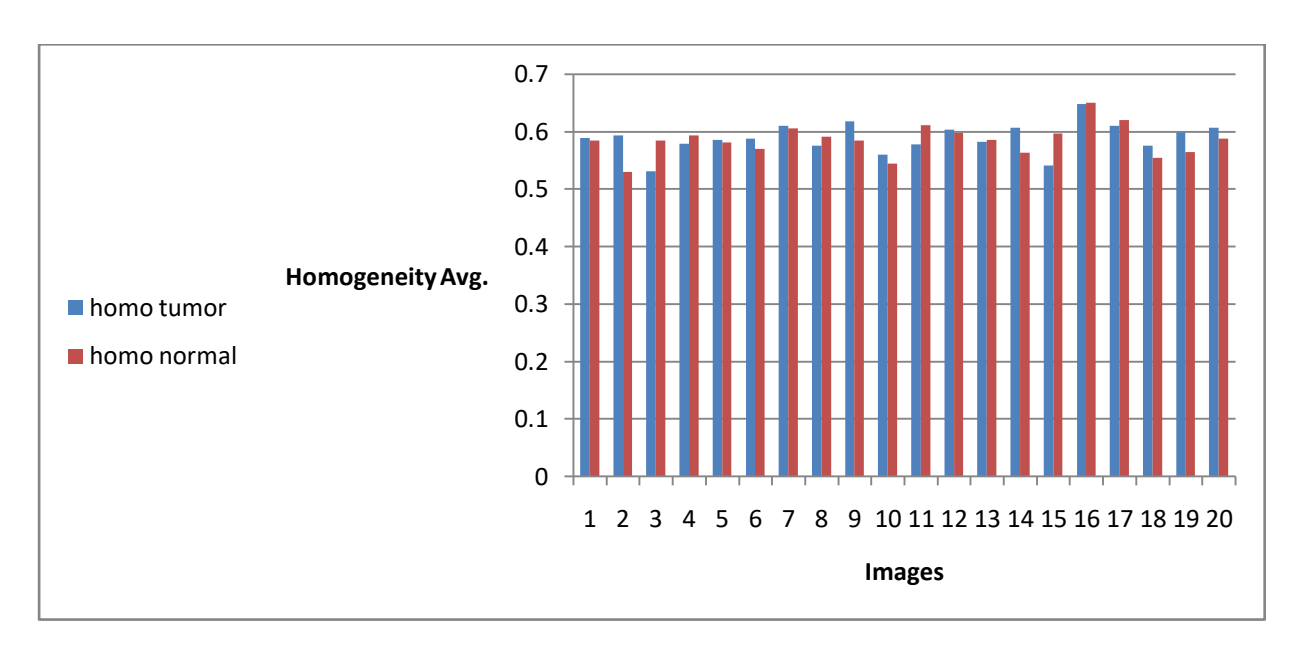


Figure 5.9 shows the Homogeneity average calculated by MATLAB code

## **Chapter six Conclusions and Recommendations**

#### 6.1 CONCLUSIONS

The difference of the interpretation of mammographic images by radiologists was very clear and the result of their diagnosis showed a marked variation in size and number of tumors.

The analysis of tables and the differences in the reading and its scatter show it's not possible to locate exactly the place of the tumor and its spread using the Haralick method. This difficulty can be attribute to the technical problems of taking the mammogram shots, the size of the frame, the age of the patient, his health condition and body size, so another features needed to increase the accuracy of the system.

#### **6.2 RECOMMENDATIONS**

- 1. The variation of the specialist diagnosis show that there is a need to Ultrasound techniques for tumor location and it spread.
- 2. It's recommended that increasing the number of samples for analysis can give better results.
- 3. Using another features or combination feature to increase the accuracy of the system.
- 4. Decreasing the size of the frame to increase the accuracy of the image analysis.

#### REFERENCES

- 1. <a href="http://www.medicalnewstoday.com/articles/37136.php">http://www.medicalnewstoday.com/articles/37136.php</a> (2015).
- 2 H.D. Cheng., X.C., Xiaowei Chen, Liming Hu, Xueling Lou, Computer-Aided Detection and Classification of Microcalcifications in Mammograms: a Survey. Pattern Recognition, 2003.
- 3. <a href="http://ww5.komen.org/BreastCancer/TheBreast.html">http://ww5.komen.org/BreastCancer/TheBreast.html</a>. (accessed 2015).
- 4.http://www.ameda.com/breastfeeding/anatomy-physiology (2015).
- 5.http://www.diagnijmegen.nl/index.php/Earlierdetection\_of\_breast\_cancer\_by\_compute r\_assisted\_decision\_making(2015) .
- 6.http://www.breastcancer.org/symptoms/testing/types/mammograms/tes (2015).
- 7. Alnazier Osman.Hamza, Maha D.El-sanosi, Asma K.Habbani, Nada A.Mustafa, and Mohamed O.Khider, Computer- aided detection of benign tumors of the female breast ,University of Medical Science and Technology, Khartoum, Sudan. Journal of clinical Engineering, 2013.
- 8.ine.org/breast\_center/treatments\_services/breast\_cancer\_screening/digital\_mammoghy( 2015).
- 9. McGill Faculty of Medicine, Interactive Mammography Analysis Web Tutorial, http://sprojects.mmi.mcgill.ca/Mammography
- 10. per Skaane, Ashwini Kshirsagar, Sandra Stapleton, Kari Young, RonaldA.Castellino, Effect of Computer-Aided Detection on Independent Double Reading of Paired Screen-Film and Full-Field Digital ScreeningMammograms.
- 11.http://www.fp.ucalgary.ca/mhallbey/what\_is\_texture.html (2015).
- 12. Erasmus Mundus Master, Texture Characterization based onGrey-Level Cooccurrence Matrix, University Jean Monnet, Saint-Etienne, France, ana.gebejes@gmail.com.
- 13. Paul Taylor, J.F., Andrew Todd-Pokropek, A Model for Integrating Image Processing Into Decision Aids for Diagnostic Radiology. Artificial Intelligence in Medicine, 1997.
- 14. Jimmy Roehrig, R.A.C., The Promise of Computer Aided Detection in Digital Mmmography. European Journal of Radiology, 1997.

- 15. Christiane Marx, Ansgar Malich, Mirjam Facius, Uta Grebenstein, Dieter Sauner, Stefan O.R. Pfleiderer, Werner A. Kaiser, Are Unnecessary Follow-up Procedures Induced by Computer-Aided Diagnosis (CAD) in Mammography Comparison of Mammographic Diagnosis With and Without Use of CA European Journal of Radiology, 2004
- 16. Bin Zheng, P., Ratan Shah, MD, Luisa Wallace, MD, Christiane Hakim, MD, Marie A. Ganott, MD, David Gur, ScD, Computer-aided Detection in Mammography: An Assessment of Performance on Current and Prior Images. Academic Radiology, 2002.
- 17. Alnazier Osman.Hamza, , Mohamed Elfadil Mohamed , Fatehia Bushara Garma, , Maha Abd Elhady Almona, , Mihad Mahmood Bakryumors ,Detection of Breast Cancer Cells by Using Texture Analysis, .Journal of clinical Engineering, 2013.
- 18. Rotation Invariant Texture Classification. p. 8-29.
- 19. Tomasz Arod'za, M.K., Erik O.D. Sevreb, David A. Yuenb, Pattern Recognition Techniques for Automatic Detection of Suspicious-Looking Anomalies in Mammograms. Computer Methods and Programs in Biomedicine, 2005.
- 20. Michael Mavroforakis, H.G., Nikos Dimitropoulos, Dionisis Cavouras, Sergios heodoridis, Significance Analysis of Qualitative Mammographic Features, Using Linear Classifiers, \_eural \_etworks and Support Vector Machines. European Journal of Radiology, 2005.
- 21. Bradley M. Hemminger, Shuquan Zong, Keith E. Muller, Christopher S. Coffey, Marla C. DeLuca R. Eugene Johnston, Etta D. Pisano. Improving the Detection of Simulated Masses in Mammograms through Two Different Image-processing Techniques. Academic Radiology, 2001. 8: p. 623-628.
- 22. Mammographic Image Analysis Society http://peipa.essex.ac.uk/ipa/pix/mia(2015).